Organic & Biomolecular Chemistry

Cytochrome c-poly(acrylic acid) conjugates with improved peroxidase turnover number

Journal:	*Organic & Biomolecular Chemistry*
Manuscript ID	OB-ART-03-2019-000541.R1
Article Type:	Paper
Date Submitted by the Author:	24-Mar-2019
Complete List of Authors:	Benson, Kyle; University of Connecticut, Chemistry Gorecki, Joseph; University of Connecticut, Chemistry Nikiforov, Anton; University of Connecticut, Chemistry Tsui, William; University of Connecticut, Chemistry Kasi, Rajeswari; University of Connecticut, Chemistry and Polymer Program, IMS Kumar, Challa; University of Connecticut, Chemistry, Institute of Materials Science, Molecular and Cell Biology

ARTICLE

Cytochrome *c*-poly(acrylic acid) conjugates with improved peroxidase turnover number

Received 00th January 20xx,
Accepted 00th January 20xx

DOI: 10.1039/x0xx00000x

K. R. Benson,[a] J. Gorecki,[a] A. Nikiforov,[a] W. Tsui,[a] R. M. Kasi,[a,b] C. V. Kumar*[,a,b,c]

Cytochrome *c*-poly(acrylic acid) (cyt *c*-PAA) conjugates with 34-fold enchancement in peroxidase turnover number (k_{cat}) are reported. Cyt *c*-PAA conjugates were prepared by carbodiimide coupling. PAA with molecular weight (M_w) ranging from 1.8k to 250k g mol^{-1} were employed, and the effect of PAA M_w on peroxiodase kinetics was assessed. The k_{cat} value increased with increased M_w of PAA, ranging from 0.077(±0.002) s^{-1} in the absence of PAA to 2.66(±0.08) for the conjugate of cyt *c* with 250k PAA. Enzymatic activity studies over pH 6-8 indicated improved activity for cyt *c*-PAA conjugates at neutral or slightly alkaline pH. Examination of the cyt *c* heme spectroscopy in the presence of H_2O_2 revealed that formation of Compound III, a reactive intermediate that leads to enzyme inactivation, was supressed in cyt c-PAA conjugates. Thus, we suggest the k_{cat} enhancement can be attributed to acidification of the pH microenvironment and inhibition of the formation of a reactive intermediate that deactivates cyt *c* during the catalytic cycle.

Introduction

Conjugation of synthetic or natural polymers to enzymes is a proven strategy to improve the thermal and chemical stability of enzymes.[1] The use of polymeric materials, particularly polyelectrolytes, to engineer the protein microenvironment is emerging as an effective means to manipulate the catalytic activity of enzyme-polymer conjugates, and can be viewed as a type of synthetic post-translational modification.[1,2] For example, the ability of polyelectrolytes to sequester ionic species can influence the local pH,[3] which has been shown to improve the activity of cytochrome *c* (cyt *c*),[4] trypsin,[5] and chymotrypsin[5] in a broad range of bulk solution pH. Non-covalent binding of substrate or inhibitor molecules to conjugated polymers can influence catalytic rates by enriching local concentrations of these species, as demonstrated with horseradish peroxidase-DNA,[6] chymotrypsin-poly(quaternary ammonium),[7] and catalase-poly(acrylic acid) conjugates.[8] The polyanionic surfaces of DNA nanocages significantly improved turnover number of several encapsulated enzymes.[9] Finally, local charge supplied by grafted polyelectrolytes can affect the catalytic cycle of trypsin by perturbing the free energy of reactants and intermediates.[5]

The above insights demonstrate that controlling the enzyme microenvironment of polymer conjugates deserves further research. We have previously demonstrated that conjugation to PAA improves the thermal and chemical stability of enzymes.[8,10] The effect of PAA molecular weight and polyelectrolyte features on the catalytic activity of enzymes has not been examined. For this reason cytochrome c-poly(acrylic acid) (cyt *c*-PAA) conjugates were selected as our model system: (1) The cyt *c* catalytic cycle features several cationic and anionic intermediates,[11,12] (2) the influence of polyelectrolytes on the relative stability of these intermediates, and their mechanistic influence enzyme turnover has not been explored and (3) the effect of PAA molecular weight and cyt *c*:COOH ratio on the kinetics of the resulting conjugates may be examined, which is an often overlooked design consideration. With these factors in mind, we report here cyt *c*-PAA conjugates with up to 34-fold enhancement in turnover number (k_{cat}), afforded by PAA

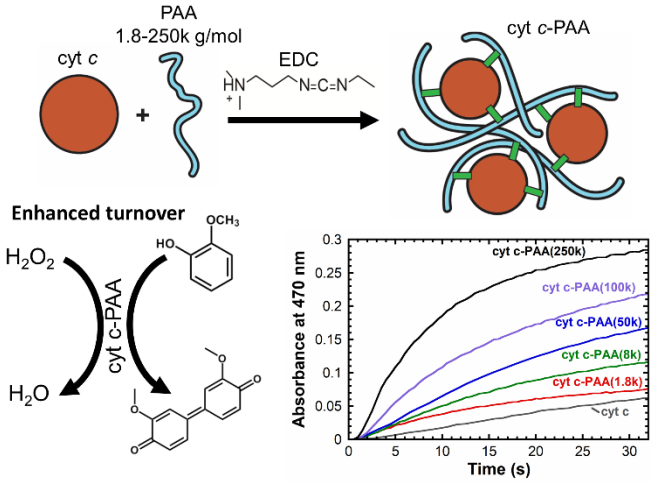

Figure 1. Synthesis of cyt *c*-PAA by EDC chemistry (top). Conjugates showed enhanced peroxidase activity, tracked by the conversion of guaiacol (200 µM) to 3,3'-dimethoxy-4,4'-biphenoquinone (λ_{max} = 470 nm).

[a] Department of Chemistry, University of Connecticut, Storrs, Connecticut 06239
[b] Institute of Materials Science, University of Connecticut, Storrs, Connecticut 06239
[c] Department of Molecular and Cell Biology, University of Connecticut, Storrs, Connecticut, 06239

† Footnotes relating to the title and/or authors should appear here.
Electronic Supplementary Information (ESI) available: [details of any supplementary information available should be included here]. See DOI: 10.1039/x0xx00000x

influence on the pH microenvironment and PAA charge-induced destabilization of wasteful reaction intermediates.

Results and Discussion

Cyt *c* is a 12.5 kDa soluble, globular hemoprotein found in mitochondria, where it shuttles electrons during respiration and acts as a peroxidase during apoptosis.[13] Cyt *c*-PAA conjugates were formed by crosslinking PAA carboxyl groups with the 20 primary amines of cyt *c* (19 lysine, 1 N-terminus)[14] using carbodiimide chemistry (**Figure 1**). PAA (10 μM) was activated by stirring with 1-ethyl-3-(3-dimethylaminopropyl)carbodiimide (EDC, 5-10 mM) in sodium phosphate buffer (20 mM, pH 7.0) for 10 minutes at 25 °C. Cyt *c* (10 μM) was then added, and the solution was stirred for four hours. Conjugates were successfully produced using PAA with average molecular weights (M_w) 1.8k, 8k, 50k, 100k, and 250k g mol^{-1}. Reaction by-products were routinely removed by dialysis. Cytochrome *c*-poly(acrylic acid) conjugates were named as cyt *c*-PAA(XXX), where the value denoted by XXX gives the molecular weight of PAA. For example, the conjugate of cyt *c* with 250k g mol^{-1} PAA is indicated by cyt *c*-PAA(250k).

Successful conjugation was validated by sodium dodecyl sulfate polyacrylamide electrophoresis (SDS-PAGE, 12.5% polyacrylamide), after analysis by agarose gel electrophoresis proved inconclusive (**Figure S1**). All cyt *c*-PAA derivatives showed several bands or wide smears, indicating the broad molecular weight distribution expected from protein-polymer nanogels.[8] The disappearance of bands corresponding to free cyt *c* confirmed the covalent conjugation to cyt *c*.

The degree of crosslinking between cyt *c* and PAA was estimated using the trinitrobenzene sulfonic acid (TNBSA) assay to quantitate the primary amines in cyt *c* and cyt *c*-PAA (**Figure S2**).[15] After conjugation to PAA, the number of primary amines of cyt *c* was reduced from 22.9(±0.8) to 10-13 (**Table S1**) for all cyt *c*-PAA conjugates. No significant difference was found among the cyt *c*-PAA with different M_w PAA (Welch's t-test, $p<0.05$). Thus, ~10 crosslinks were made per cyt *c* during the EDC condensation.

Next, we assessed the effect of PAA conjugation on cyt *c* peroxidase kinetics. In the catalytic cycle, hydrogen peroxide is reduced to water, and single electron oxidation of two equivalents of guaiacol regenerates the ferric heme state. These two guaiacol radicals combine to form 3,3'-dimethoxy-4,4'-biphenoquinone, which is orange in color (**Figure 1**).[16] Oxidation of guaiacol is the rate determining step of peroxidase activity, so the Michaelis-Menten kinetics were examined by varying the [guaiacol] (1-200 μM) for a fixed [H_2O_2] (50 mM).[17] The constants K_M and v_{max} of cyt *c* and cyt *c*-PAA of all molecular weights were obtained by fitting the Michaelis-Menten model to the guaiacol-dependent initial rate data. The non-linear least squares fits are represented by the dashed lines in **Figure 2**. The K_M value of cyt *c* for guaiacol oxidation was 7(±1) μM, orders of magnitude smaller than that of other heme enzymes but in good agreement with literature reports.[17] The K_M values of cyt *c*-PAA(1.8k), cyt *c*-PAA(8k), and cyt *c*-PAA(50k) did not differ significantly (Welch's t-test, $p<0.05$) from cyt *c*, but K_M increased with larger molecular weight PAA, reaching up to 38(±4) μM.

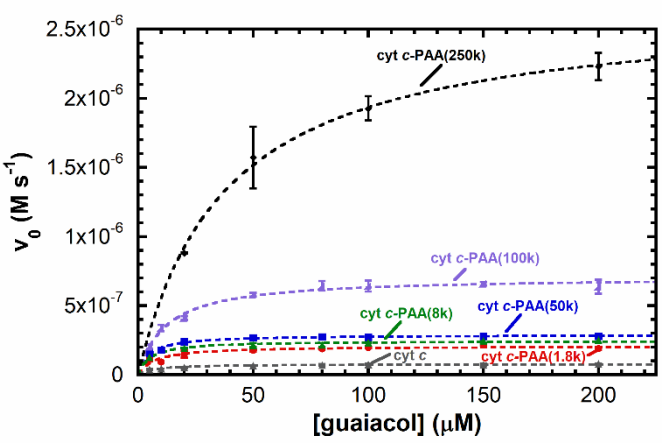

Figure 2. Michealis-Menten kinetics of cyt *c*-PAA.

	K_M (M)	k_{cat} ($M s^{-1}$)
cyt *c*	7(±1)x10^{-6}	0.077(±0.002)
cyt *c*-PAA(1.8k)	7(±2)x10^{-6}	0.21(±0.01)
cyt *c*-PAA(8k)	5.1(±0.9)x10^{-6}	0.245(±0.005)
cyt *c*-PAA(50k)	4.8(±0.5)x10^{-6}	0.289(±0.004)
cyt *c*-PAA(100k)	12(±1)x10^{-6}	0.71(±0.016)
cyt *c*-PAA(250k)	38(±4)x10^{-6}	2.66(±0.08)
cyt *c*/PAA(50k)	6.8(±0.9)x10^{-6}	0.285(±0.004)
cyt *c*/PAA(100k)	10(±1)x10^{-6}	0.281(±0.006)
cyt *c*/PAA(250k)	9(±3)x10^{-6}	0.29(±0.01)

Table 1. Michealis-Menten parameters of cyt *c*-PAA covalent conjugates and cyt *c*/PAA physical mixtures (shaded cells)

The turnover number (k_{cat}) is the rate constant for conversion of enzyme-substrate complex to product, and was determined using the fitted v_{max}. For native cyt *c*, k_{cat} was 0.077(±0.002) s^{-1}, again in good agreement with literature reports.[17] As molecular weight of PAA increased, k_{cat} of cyt *c*-PAA increased as well, ranging from 0.21(±0.01) s^{-1} in the case of cyt *c*-PAA(1.8k) to 2.66(±0.08) s^{-1} for cyt *c*-PAA(250k). This represented a dramatic increase in the enzymatic activity of cyt *c* after conjugation to PAA, with the forward rate constant enhanced between 3- and 34-fold.

Physical mixtures of cyt *c* and PAA 50k, 100k, and 250k (no EDC) were examined next to determine if covalent conjugation was required for activity enhancements (**Figure S3**). The physical mixture of cyt *c* and 50k M_w PAA had a similar k_{cat} to the covalent adduct, which was ~4-fold greater than that of cyt *c* alone. Agarose gel electrophoresis of cyt c/PAA physical mixtures demonstrated strong non-covalent complexation of cyt c and PAA (**Figure S1A**), so the enhanced activity of these species was expected. Unlike the covalent conjugates, no further enhancement was noted with 100k or 250k M_w PAA physical mixtures. The full complement of Michaelis-Menten parameters for cyt *c*-PAA and cyt *c*/PAA physical mixtures are in **Table 1**.

The enhancement of cyt *c* peroxidase activity upon binding anionic cardiolipin has been well documented in the literature. However, partial unfolding of cyt *c* and dissociation of the Fe-Met80 bond are key to the enhanced peroxidase activity in the presence of cardiolipin.[13] A ~6-fold increase in k_{cat} for the

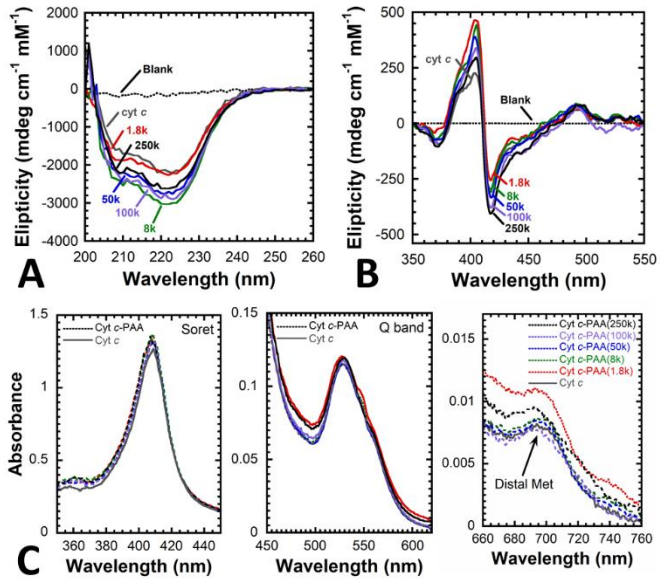

Figure 3. (A) UV circular dichroism (CD) spectra of cyt *c* and cyt *c*-PAA conjugates. Conjugate spectra are labelled with their corresponding PAA molecular weight. (B) Soret CD spectra of cyt *c* and cyt *c*-PAA conjugates. (C) Soret (left), Q band (center), and Met charge transfer band (right) absorbance spectra of cyt *c* (solid curve) and cyt *c*-PAA conjugates (dashed lines).

oxidation of guaiacol has also been reported for horse cyt *c* dimerized by treatment with ethanol,[17] while binding to CTAB decorated gold nanoparticles increased k_{cat} of pyrogallol oxidation ~14-fold.[18] Binding to functionalized carbon nanomaterials increased v_{max}/K_M dramatically.[19] Again, these rate enhancements by others are accompanied by the breakage of the Met80-Fe bond and/or partial denaturation of cyt *c*. Thus, we examined cyt *c*-PAA to determine if the heme ligation had been affected by the conjugation reaction.

Circular dichroism (CD) and visible absorbance spectroscopy were employed to determine if the k_{cat} enhancement was caused by changes to cyt *c* secondary structure or heme ligation. Cyt *c* is primarily alpha helical, which was reflected in the UV CD by negative peaks at 222 and 208 nm (**Figure 3A**).[20] The 208 nm band was weaker than the 222 nm band in all cases, indicative of monomeric cyt *c*.[21] Only small changes in molar ellipticity were observed, demonstrating that there was little perturbation in the protein secondary structure. Similar changes were observed in the CD spectra of cyt *c*/PAA mixtures lacking EDC, as well as in experiments where cyt *c* and PAA were placed in separate cells and measured in tandem (**Figure S4**). These data suggest the observed changes in the CD spectra of cyt *c*-PAA could simply be artifacts caused by PAA absorbance in the UV.

The spectra of the heme prosthetic group are highly sensitive its ligation and binding pocket structure, which are reflected in the Soret band (~400 nm) and Q band (~550 nm).[22,23] The spectra of all cyt *c*-PAA samples in these regions could be nearly overlaid on that of native cytochrome c, clearly demonstrating that the conjugation reaction only minimally perturbed the sensitive structure of the protein (**Figure 3B-C**). The Soret CD spectra of cyt *c* and all cyt *c*-PAA derivatives showed a negative peak at 415 nm and a positive peak at 398 nm, indicative of native ferric cyt *c* with His/Met in the axial positions.[24] The Soret band of native ferric cyt *c* has a maximum at 409 nm in the visible absorbance spectrum,[22,23] which was observed in all cyt *c*-PAA except cyt *c*-PAA(250k). The Soret band of cyt *c*-PAA(250k) shifted to 407 nm, which could be caused by minor changes in the secondary structure.[22] The Q band of native cyt *c* had a maximum at 528 nm, which was maintained in all cyt *c*-PAA derivatives. Finally, a weak charge transfer band at 695 nm demonstrated the native ligation of His/Met for cyt *c* and all cyt *c*-PAA.[25] Taken together, the data indicated that the secondary structure and heme ligation of cyt *c*-PAA was not significantly changed and thus not responsible for the enhancement in k_{cat}.

The influence of anionic polyelectrolytes on enzyme activity by controlling the microenvironment may provide insight into the enhanced kinetics of cyt *c*-PAA. For example, encapsulation of enzymes such as glucose oxidase in polyanionic DNA nanocages enhanced the catalytic activity.[9] Glucose oxidase and horseradish peroxidase bound to DNA exhibit increased cascade reaction efficiency because the phosphate backbone maintains a favorable local pH.[26] Additionally, conjugation of cyt *c* to poly(methacrylic acid) was reported to change the optimum pH of cyt *c* by acidifying the pH microenvironment.[4] We also studied local enrichment of guaiacol by partitioning to the PAA phase, but guaiacol appeared to have only weak affinity for PAA (**Figure S5**).

To test the effect of PAA on the pH activity profile, we measured the rate of guaiacol oxidation (200 µM guaiacol, 50 mM H_2O_2, 20 mM sodium phosphate) at pH 6-8. Cyt *c* and cyt *c*-PAA(50k) were examined in this manner. The peroxidase activity of cyt decreased as the pH was increased, while the pH profile of cyt *c*-PAA was relatively flat (**Figure 4**). The Soret CD and absorbance spectra did not change over this pH range, indicating no changes to heme ligation (**Figure S6**). These observations were in line previously reports of cyt *c*-PMMA conjugates with broadened pH response.[4] Thus, modulation of the local pH by the weakly acidic COOH groups of PAA may explain enhanced activity of cyt *c*-PAA.

Examining the catalytic cycle of cyt *c* revealed an additional mechanism for improved catalysis by cyt *c*-PAA (**Figure 5A**). In heme peroxidases, oxidation of guaiacol by occurs in three

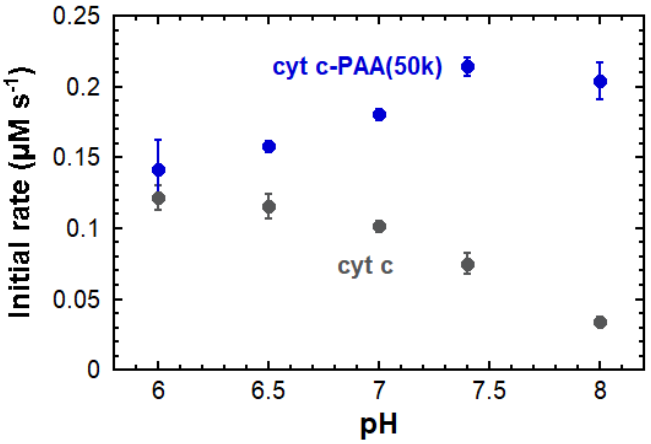

Figure 4. Variation of cyt *c* and cyt *c*-PAA(50k) rate of guaiacol oxidation with pH. Activity of cyt *c* decreased as pH increased, while that of cyt *c*-PAA increased over the same range.

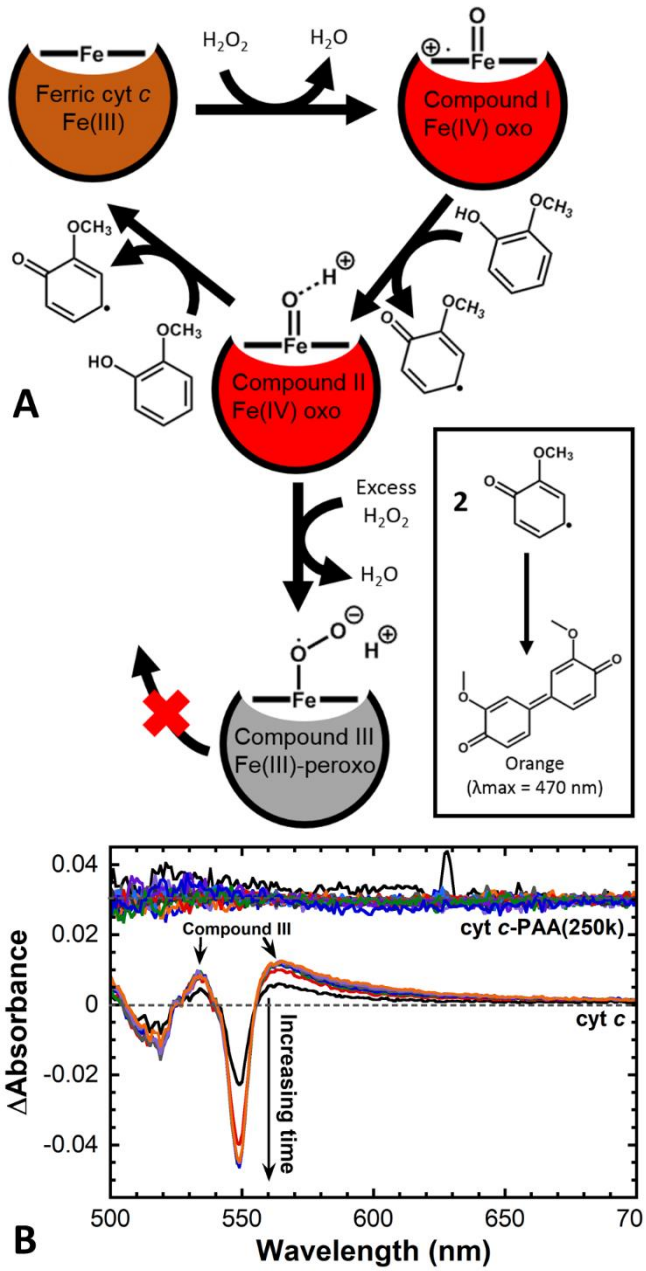

Figure 5. (A) Schematic representation of cyt *c* catalytic cycle. (B) Change in Q-band absorbance of cyt *c* and cyt *c*-PAA(250k) (offset) in the presence of 100 μM H_2O_2.

steps.[11,12] First, H_2O_2 is reduced and the heme iron is oxidized from Fe(III) to Fe(IV)-oxo (Compound I). Next, the oxidation of guaiacol produces a guaiacol radical and converts the heme to Compound II, which is still in the Fe(IV) state. Finally, oxidation of a second equivalent of guaiacol converts the heme back to the native ferric state.[11] Critically, Compound II can react with H_2O_2 to produce Compound III, a negatively charged Fe(III)-peroxo state. Formation of Compound III can be reversible, but reaction of Compound III with peroxide results in enzyme inactivation by auto-oxidation and heme bleaching.[12] Even when the enzyme is not inactivated, Compound III is a "sink" for guaiacol oxidation, as it consumes an equivalent of hydrogen peroxide and completes a catalytic cycle without a concomitant oxidation of guaiacol.

We hypothesized that the high negative charge density of PAA could suppress formation of Compound III by unfavorable electrostatic interactions. It is possible that PAA charge may also stabilize the cationic Compounds I and II. However, we examined formation of Compound III because its accumulation can be conveniently observed spectroscopically without time-resolved techniques under the appropriate conditions.[12,27,28] To rationalize the interaction of charged groups of PAA with heme reactive intermediates, we estimated the Debye length in 20 mM sodium phosphate buffer at room temperature.[29] Under these conditions, the Debye length was ~1.6 nm, comparable to the diameter of cyt *c*. Thus, it was reasonable to expect electrostatic interaction between PAA charged groups and reactive heme intermediates.

We examined the formation of Compound III by monitoring the Q bands of cyt *c* and cyt *c*-PAA(250k) in the presence of 100 μM H_2O_2. (**Figure 5B**, **Figure S7**). Upon introduction of 100 μM H_2O_2 to a solution of 10 μM cyt *c* (20 mM sodium phosphate, pH 7.0), the shoulder at 550 nm disappeared while the absorbance at 533 nm and 563 nm increased, which indicate the appearance of Compound III.[17] These spectral changes were complete within 30 seconds, and persisted for more than 30 minutes. Subsequent addition of guaiacol did not produce 3,3'-dimethoxy-4,4'-biphenoquinone, which suggests that the catalyst was deactivated. Under similar conditions, cyt *c*-PAA(250k) did not show any spectral changes to indicate the appearance of Compound III.

Next, heme bleaching studies were conducted to examine the inactivation of cyt *c* and cyt *c*-PAA under the conditions of the kinetic assays (20 mM sodium phosphate, pH 7.0, 20 °C). Cyt *c* and cyt *c*-PAA(250k) were exposed to 50 mM H_2O_2, and the disappearance of the Soret absorbance at 410 nm was monitored. Interestingly, heme bleaching of cyt *c*-PAA(250k) was initially more rapid that that of cyt *c* (**Figure S8A**). However, as the reaction proceeded, the rate of cyt *c*-PAA(250k) bleaching slowed relative to cyt *c*. After the reaction was complete, cyt *c*-PAA(250k) retained 13.1(±0.9)% of its intial Soret absorbance, while cyt *c* retained only 6(±1)% (**Figure S8B**). In the absence of guaiacol, conjugation to PAA offered mild protection from inactivation by heme bleaching. Inactivation by peroxide is further inhibited by the presence of substrates guaiacol or phenol,[28] so this gain in stability can be relevant during guaiacol oxidation.

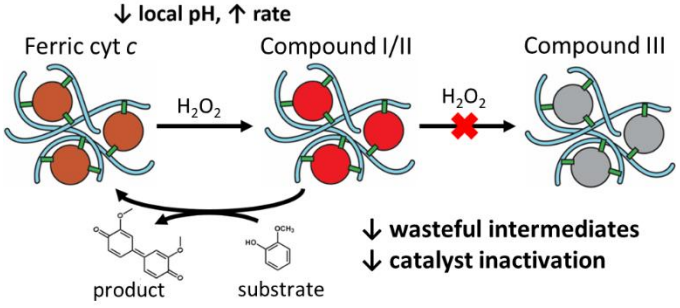

Scheme 1. Schematic representation of dual influences of PAA on cyt *c* peroxidase activity.

Taken together, the modulation of local pH and suppression of wasteful intermediates could have a synergistic effect, which result in the 34-fold enhancement in cyt *c*-PAA turnover number reported here (**Scheme 1**). This may also help to explain the broadened pH profile, as the ionization of PAA changes >50% over the range studied.[30] Additionally, both effects explain the dependence of k_{cat} on PAA M_w – increasing the M_w at a fixed cyt *c*:PAA mole ratio increases the concentration of acidic groups and magnitude of the negative charge.

We next examined if these concepts could be extended to other heme peroxidases, such as horseradish peroxidase (HRP) or hemoglobin (Hb). PAA conjugates of HRP and Hb were prepared and characterized in a similar manner to cyt *c*-PAA, after which Michaelis-Menten kinetics of guaiacol oxidation were measured (**Figure S9, Table S2**). HRP-PAA had similar K_M and k_{cat} to native HRP (Welch's t-test, $p<0.05$). The rate constant of inactivation of HRP by H_2O_2 via Compound III is at least 10-fold smaller than that of cyt *c*,[31,32] so the lack of improvement was not unexpected. Hb, a typically inefficient peroxidase,[33] was improved by conjugation to PAA. k_{cat} of Hb-PAA(50k) and Hb-PAA(250k) were 1.1(±0.1) s^{-1} and 0.62(±0.04) s^{-1}, both larger than that of Hb, 0.43(±0.06) s^{-1} (**Table S2**). Together, the kinetics of HRP-PAA, cyt *c*-PAA, and Hb-PAA indicated that the PAA could improve the efficiency of certain enzymatic processes when the enzymes were unstable in the presence of excess H_2O_2.

Conclusions

The results presented here hint at ways in which the physical characteristics of polyelectrolytes such as PAA could be used to tune the catalytic activity and efficiency of enzyme-polymer conjugates. In this case, PAA destabilized a wasteful intermediate while acidifying the local pH, thus improving the activity of heme peroxidases, cyt *c* and Hb, and leading to the 34-fold increase in k_{cat} of cyt *c*-PAA(250k). Significantly, by supressing Compound III formation, PAA influenced the enzyme mechanism. These effects could be systematically controlled by varying the PAA M_w, allowing for precise tuning of peroxidase activity. Additionally, these findings suggest that, with a good understanding of the catalytic mechanism and careful polymer selection, this concept could be extended to other enzyme-polymer systems.

Experimental

Full experimental details are provided in the Supporting Information.

Supporting Information

Supplementary figures and experimental methods can be found in the Supporting Information.

Conflicts of interest

There are no conflicts to declare.

Acknowledgements

This work was supported by NSF EAGER Award DMR-1441879 and by UCONN VPR Research Excellence Award. The authors thank Dr. Yao Lin, Jill Durso, Tawan Jamdee, Sabika Sherwani, Deaneira Lakheram, and Caterina Riccardi for assistance.

References

1 T. A. Wright, R. C. Page and D. Konkolewicz, *Polym. Chem.*, 2019, **10**, 434–454.
2 I. Cobo, M. Li, B. S. Sumerlin and S. Perrier, *Nat Mater*, 2015, **14**, 143–159.
3 R. Klitzing and H. Moehwald, *Langmuir*, 1995, **11**, 3554–3559.
4 Y. Zhang, Q. Wang and H. Hess, *ACS Catal.*, 2017, **7**, 2047–2051.
5 L. Goldstein, *Biochemistry*, 1972, **11**, 4072–4084.
6 Y. Gao, C. C. Roberts, J. Zhu, J.-L. Lin, C. A. Chang and I. Wheeldon, *ACS Catal.*, 2015, **5**, 2149–2153.
7 H. Murata, C. S. Cummings, R. R. Koepsel and A. J. Russell, *Biomacromolecules*, 2014, **15**, 2817–2823.
8 C. M. Riccardi, K. S. Cole, K. R. Benson, J. R. Ward, K. M. Bassett, Y. Zhang, O. V. Zore, B. Stromer, R. M. Kasi and C. V. Kumar, *Bioconjug. Chem.*, 2014, **25**, 1501–1510.
9 Z. Zhao, J. Fu, S. Dhakal, A. Johnson-Buck, M. Liu, T. Zhang, N. W. Woodbury, Y. Liu, N. G. Walter and H. Yan, *Nature Communications*, 2016, **7**, 10619.
10 C. M. Riccardi, D. Mistri, O. Hart, M. Anuganti, Y. Lin, R. M. Kasi and C. V. Kumar, *Chem. Commun.*, 2016, **52**, 2593–2596.
11 G. I. Berglund, G. H. Carlsson, A. T. Smith, H. Szöke, A. Henriksen and J. Hajdu, *Nature*, 2002, **417**, 463–468.
12 B. Valderrama, M. Ayala and R. Vazquez-Duhalt, *Chemistry & Biology*, 2002, **9**, 555–565.
13 Y.-W. Lin and J. Wang, *Journal of Inorganic Biochemistry*, 2013, **129**, 162–171.
14 G. W. Bushnell, G. V. Louie and G. D. Brayer, *J. Mol. Biol.*, 1990, **214**, 585–595.
15 A. F. Habeeb, *Anal. Biochem.*, 1966, **14**, 328–336.
16 D. R. Doerge, R. L. Divi and M. I. Churchwell, *Analytical Biochemistry*, 1997, **250**, 10–17.
17 Z. Wang, T. Matsuo, S. Nagao and S. Hirota, *Org. Biomol. Chem.*, 2011, **9**, 4766–4769.
18 S. Maiti, K. Das, S. Dutta and P. K. Das, *Chemistry – A European Journal*, **18**, 15021–15030.
19 M. Patila, I. V. Pavlidis, E. K. Diamanti, P. Katapodis, D. Gournis and H. Stamatis, *Process Biochemistry*, 2013, **48**, 1010–1017.
20 N. J. Greenfield, *Nat Protoc*, 2006, **1**, 2876–2890.
21 S. Hirota, Y. Hattori, S. Nagao, M. Taketa, H. Komori, H. Kamikubo, Z. Wang, I. Takahashi, S. Negi, Y. Sugiura, M. Kataoka and Y. Higuchi, *PNAS*, 2010, **107**, 12854–12859.
22 S. Oellerich, H. Wackerbarth and P. Hildebrandt, *J. Phys. Chem. B*, 2002, **106**, 6566–6580.
23 E. Stellwagen, *Biochemistry*, 1968, **7**, 2893–2898.
24 M. Simon, V. M.-L. Meuth, S. Chevance, O. Delalande and A. Bondon, *J Biol Inorg Chem*, 2013, **18**, 27–38.
25 L. S. Kaminsky, V. J. Miller and A. J. Davison, *Biochemistry*, 1973, **12**, 2215–2221.
26 Y. Zhang, S. Tsitkov and H. Hess, *Nature Communications*, 2016, **7**, 13982.
27 S. A. Adediran, *Archives of Biochemistry and Biophysics*, 1996, **327**, 279–284.

28 K. J. Baynton, J. K. Bewtra, N. Biswas and K. E. Taylor, *Biochimica et Biophysica Acta (BBA) - Protein Structure and Molecular Enzymology*, 1994, **1206**, 272–278.
29 R. Tadmor, E. Hernández-Zapata, N. Chen, P. Pincus and J. N. Israelachvili, *Macromolecules*, 2002, **35**, 2380–2388.
30 T. Swift, L. Swanson, M. Geoghegan and S. Rimmer, *Soft Matter*, 2016, **12**, 2542–2549.
31 J. A. Villegas, A. G. Mauk and R. Vazquez-Duhalt, *Chem. Biol.*, 2000, **7**, 237–244.
32 S. A. Adediran and A.-M. Lambeir, *European Journal of Biochemistry*, 1989, **186**, 571–576.
33 M. J. Smith and W. S. Beck, *Biochimica et Biophysica Acta (BBA) - Protein Structure*, 1967, **147**, 324–333.

TOC graphic

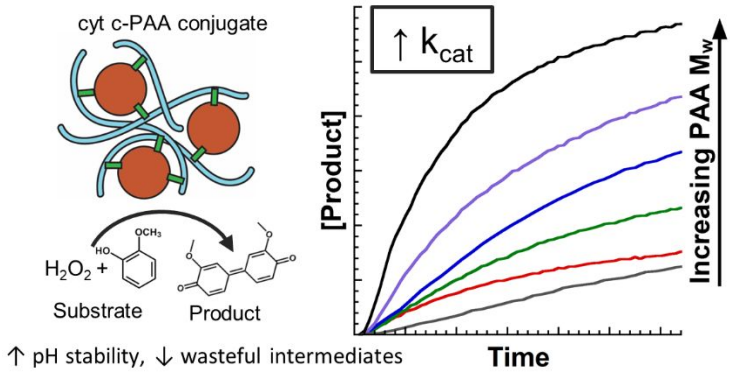

TOC text

Cytochrome *c*-poly(acrylic acid) conjugates with 34-fold enhanced peroxidase activity due toacidification of enzyme microenvironment and suppression of wasteful intermediates.